VHCF response of AISI H13 steel: assessment of size effects through Gaussian specimens

Available online at www.sciencedirect.com

ScienceDirect

Procedia Engineering 109 (2015) 121 – 127

Procedia Engineering

www.elsevier.com/locate/procedia

XXIII Italian Group of Fracture Meeting, IGFXXIII

VHCF response of AISI H13 steel: assessment of size effects through Gaussian specimens

A. Tridello*, D.S. Paolino, G. Chiandussi, M. Rossetto

Department of Mechanical and Aerospace Engineering, Politecnico di Torino, Turin, Italy

Abstract

The paper aims at assessing the influence of the Size-Effect (SE) parameter on the VHCF response of the AISI H13 steel. Ultrasonic tests were performed on Gaussian and hourglass specimens characterized by different risk-volumes (volume of material subjected to an almost uniform stress amplitude). Experimental results showed that a significant difference exists between the VHCF strengths of the investigated material obtained by using specimens with different risk-volumes.

Peer-review under responsibility of the Gruppo Italiano Frattura (IGF)

Keywords: Very High Cycle Fatigue (VHCF); Gigacycle fatigue; Ultrasonic test; Gaussian specimen; size effect; inclusions.

1. Introduction

In recent years, the Very-High-Cycle Fatigue (VHCF) behavior of metallic materials gained significant attention. The increment of the required design lifetime, up to 10^{10} cycles, for structural components commonly used in different industrial fields (aerospace, mechanical and energy industry), led to a more detailed investigation on the VHCF behavior of materials.

Experimental tests carried out by using ultrasonic testing machines [1,2] showed that specimens may fail at stress amplitudes below the conventional fatigue limit. In particular, experimental results on high-strength steels showed that, depending on the stress amplitude, failures may be due to two different types of crack nucleation [1,3]. If the stress amplitude is above the conventional fatigue limit, cracks nucleate at the specimen surface (surface nucleation); if the stress amplitude is below the conventional fatigue limit, cracks nucleate from inclusions or internal defects

* Corresponding author. Tel.: +30-011-0906913;
E-mail address: andrea.tridello@polito.it

Peer-review under responsibility of the Gruppo Italiano Frattura (IGF)
doi:10.1016/j.proeng.2015.06.218

(internal nucleation). Following the experimental evidence, new phenomenological models were introduced [4] for the description of the fatigue life, in order to take into account the random occurrence of superficial and internal failures and the possible presence of a VHCF limit.

Together with the introduction of new fatigue life models, VHCF research focused on the study of the effect of different factors affecting the VHCF properties of materials. In particular, the Size-Effect (SE) factor was recently investigated [5-7]. Experimental results showed that specimen size and, in particular, specimen risk-volume (RV, volume of material subjected to a stress amplitude above the 90% of the maximum stress) significantly influences the VHCF strength of high-strength steels: the larger the RV, the larger the probability of finding larger inclusions and, in agreement with the Murakami's theory [8], the smaller the VHCF strength. Therefore, for a conservative evaluation of the VHCF strength, VHCF tests should be carried out on specimens with a RV close to the RV of components in service conditions. However, a significant increment of RV (above 1000 mm^3) is not possible with common specimen shapes (hourglass or dog-bone) used for ultrasonic tests [9,10]: limited RVs (less than $200\,mm^3$) can be tested with hourglass specimens and moderate RVs (less than $2000\,mm^3$) can be tested with dog-bone specimens.

A further increment of the RV in dog-bone specimen is prevented by the non-uniform stress distribution along the specimen part with constant cross-section. The Authors recently proposed the adoption of a new specimen shape (Gaussian specimen) that permits to test large RVs (up to $20000\,mm^3$) in ultrasonic tests [9]. The central part of the Gaussian specimen entails the Gaussian shape, which ensures a uniform stress distribution and, as a consequence, a significant increment of the tested RV.

The present paper aims at assessing the influence of the SE factor on the VHCF response of the AISI H13 steel: ultrasonic tests were performed on Gaussian specimens characterized by a large RV (about 2300 mm^3, the largest tested in the literature). Hourglass specimens with a limited RV (about 200 mm^3) were also tested. Fracture surfaces were investigated through optical and Scanning Electron Microscope (SEM) in order to analyze defects from which VHCF cracks nucleated.

Nomenclature

SE	Size-Effect
RV	Risk-volume
K_t	Stress concentration factor
ODA	Optically Dark Area
$\sqrt{area}$	square root of the projected area of the defect that originated the failure
σ_w	VHCF limit
HV	Vickers hardness
$\sqrt{area_{INC+ODA}}$	square root of the area delimited by the inclusion and the ODA
$\sigma_{w,h}$	VHCF limit estimated by testing hourglass specimens
$\sigma_{w,G}$	VHCF limit estimated by testing Gaussian specimens
$\sqrt{area_{INC}}$	square root of the inclusion area

2. Experimental material

The examined AISI H13 steel is obtained by conventional casting, formed into flat bars and subjected to a soft annealing. Tab. 1 reports the chemical composition and the standard specification of the investigated tool steel as provided by the supplier.

Commercial slabs with a 254x127 mm cross-section were used for specimen production. The slabs were cut into rectangular bars with dimensions 32x32x115 mm. Each bar was machined in order to obtain the specimens for the ultrasonic VHCF tests. Hourglass specimens characterized by a $200\,mm^3$ risk-volume and Gaussian specimens characterized by a $2300\,mm^3$ RV were manufactured (Fig. 1). Both specimens were designed in order to have a stress concentration factor K_t below 1.08 [9]. The specimen geometries are shown in Fig. 1.

Typical analysis %	C	Si	Mn	Cr	Mo	V
	0.39	1.0	0.4	5.3	1.3	0.9
Standard specification	AISI H13, W.- Nr 1.2344, EN 40CrMOV5-1					

Tab. 1. Uddeholm Orvar®: chemical composition and standard specification.

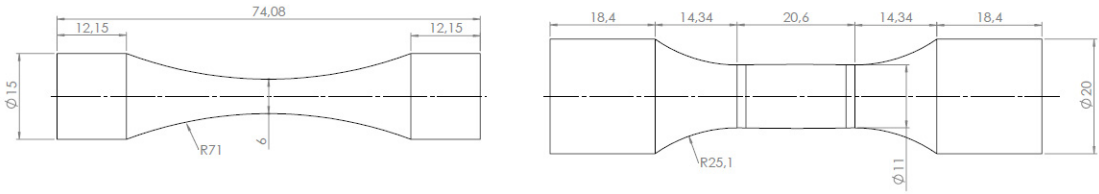

Fig. 1: Specimens used for VHCF tests: (a) hourglass specimen; (b) Gaussian specimen.

After machining, specimens were quenched and tempered with an ordinary industrial cycle, in a vacuum furnace. The heat treatment cycle was as follows: preheating at 750 °C, austenitizing at 1030 °C, gas quenching, first tempering at 520 °C, second and third tempering at 540 °C. The microstructure after the heat treatment was tempered martensite. The tensile strength and Vickers hardness of the heat treated steels were 2000 MPa and 560 HV, respectively.

In order to avoid surface nucleation of cracks due to machining defects, specimens were fine polished by using sandpapers with increasing grits (from #200 to #1200).

3. Experimental procedure

Fully reversed tension-compression tests were carried out by using the ultrasonic testing machine developed at the Politecnico di Torino [11]. Intermittent tests (pulse phase and pause phase) were carried out in order to limit the temperature increment inside the specimen. Heating of the specimen was continuously monitored during the test through an infrared temperature sensor. Vortex tubes were employed to reduce the cooling pauses and to increase the pulse duration. The specimen temperature was kept in the range between 303 K and 323 K.

Specimens were loaded at a constant stress amplitude until failure or up to 10^{10} cycles (runout specimens). A closed-loop control based on the displacement measured at the specimen free surface assured the proper application of the stress amplitude in the central specimen part. Before each VHCF characterization, a strain gauge calibration was performed in order to accurately correlate the displacement amplitude measured at the free specimen end to the stress amplitude in the Gaussian part.

4. Experimental results

Specimens were subjected to constant stress amplitudes, ranging from 570 MPa to 710 MPa in case of hourglass specimens and ranging from 490 MPa to 570 MPa in case of Gaussian specimens. Thirteen out of seventeen hourglass specimens failed during the VHCF tests at a number of cycles to failure ranging from 1.19×10^{7} cycles to 9.40×10^{9} cycles. Eleven out of thirteen Gaussian specimens failed during the VHCF tests at a number of cycles to failure ranging from 4.20×10^{7} cycles to 9.61×10^{9} cycles. Fracture surfaces were observed by means of a SEM in order to determine crack origins: all the fatigue fractures nucleated from non-metallic inclusions (oxides-types inclusions). Experimental results were analyzed in order to compare the VHCF strengths of the two specimen types.

4.1. S-N curves

The distribution of crack initiations in the RV (Fig. 2) was taken into consideration. According to Fig. 3, failures in Gaussian specimens were uniformly distributed within the RV, thus confirming the uniformity of the stress amplitude in the Gaussian specimen part. Failures in hourglass specimens were concentrated near the specimen mid-section.

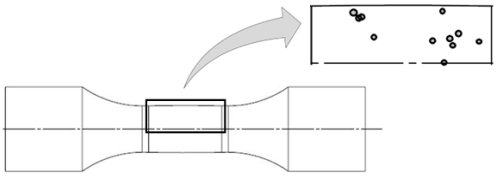

Fig. 2: Crack initiation distribution within the risk-volume of the tested Gaussian specimens.

The S-N curves for the two specimen types were obtained according to the model proposed in [4]. In particular the case "One failure mode due to one cause without fatigue limit" was considered. Parameter estimation was performed by applying the Maximum Likelihood principle. Fig. 3 plots the median S-N curves (50% probability), the 10% and the 90% S-N curves estimated from the VHCF tests on hourglass and Gaussian specimens.

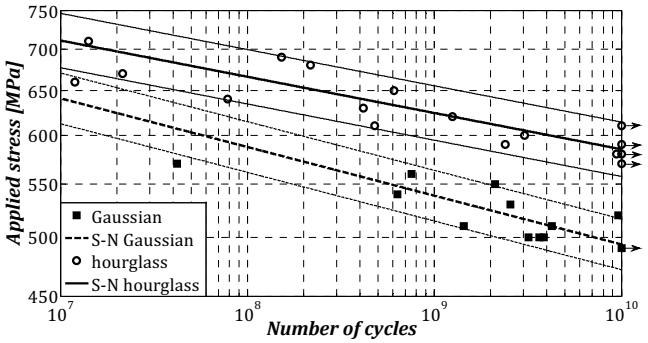

Fig. 3: 90%, 50% and 10% S-N curves obtained by testing hourglass and Gaussian specimens.

According to Fig. 3, the S-N curves of hourglass specimens lay entirely above the S-N curves of the Gaussian specimen. The difference between the curves of the two specimen types tends to increase for very high number of cycles (above 10^9 cycles). Hourglass specimens exhibit a VHCF strength at 10^{10} cycles significantly larger (about 18%) than Gaussian specimens.

4.2. Fatigue limit estimation

The defects from which cracks originated were observed through an optical microscope and were considered for the estimation of the VHCF limit according to the $\sqrt{area}$ parameter model proposed by Murakami [8]. All failures showed the typical fish-eye morphology with the Optically Dark Area (ODA) [8] around the inclusion (Fig. 4).
According to the Murakami's model [8], in case of internal nucleation of cracks from non-metallic inclusions or defects, the VHCF limit (σ_w) depends on the Vickers hardness (HV) and on the square root of the projected area ($\sqrt{area}$) of the defect that originated the failure (i.e., $\sigma_w = 1.56 \cdot (HV + 120) / \left(\sqrt{area}\right)^6$). In case of low stress

amplitude and in presence of ODA [12], the initial defect corresponds to the area delimited by the inclusion and the ODA (i.e., $\sqrt{area} = \sqrt{area_{INC+ODA}}$). The $\sqrt{area_{INC+ODA}}$ values were measured by using an optical microscope. Fig. 5 shows the interval plot for the VHCF limit estimated by considering the $\sqrt{area_{INC+ODA}}$ values measured on each fracture surface. 95% confidence interval bars for the two of H13 steels are plotted

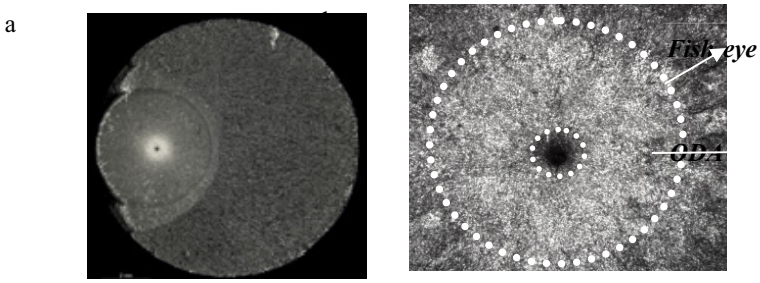

Fig. 4: Fracture surface observed through optical microscope: (a) Internal fracture; (b) Fish-eye and Optically Dark Area.

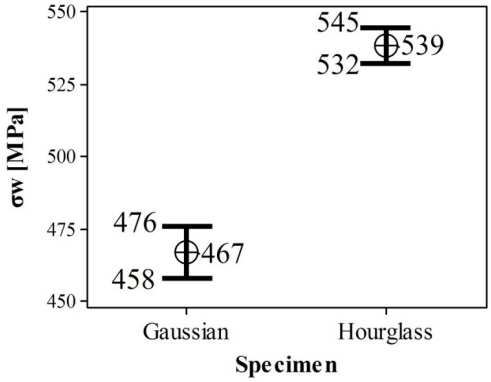

Fig. 5: Interval plot (95% confidence interval) for the VHCF limit estimated according to the Murakami's model.

According to Fig. 5, a significant difference exists between the VHCF limit estimated by testing hourglass specimens ($\sigma_{w,h}$) and the VHCF limit estimated by testing Gaussian specimens ($\sigma_{w,G}$). In particular, the mean value of $\sigma_{w,h}$, equal to 539 MPa, is significantly larger (about 15%) than the mean value of $\sigma_{w,G}$, equal to 467 MPa. Experimental results confirm the VHCF limit estimation obtained according to the Murakami's model [8]. Indeed, no failures occurred at stress amplitude below the estimated VHCF limit and the VHCF strength at 10^{10} cycles (Section 4.1) is larger than the estimated VHCF limit for both specimen types.

Therefore, a significant decrement in the VHCF strength and limit was found by testing Gaussian specimens with a large RV. VHCF tests on even larger RVs should be carried out for a proper assessment of the VHCF response at very large RVs.

4.3. *Largest inclusion size distributions*

ODAs originate around non metallic inclusions; their size depends on the applied stress amplitude and, in particular, on the size of the original inclusion [8]. Inclusion size affects ODA size and, consequently, the VHCF strength.

The statistical distributions of the largest inclusion size in the two specimen types were determined according to the procedure suggested in [8,12]. Inclusion size in runouts was measured by testing the specimens at higher stress

amplitudes up to failure. According to [8], the inclusion size was assumed to follow a Type I LEVD (i.e., the Gumbel distribution of maximum). The Gumbel plot in Fig. 6 shows the experimental data together with the estimated statistical distributions for both hourglass and Gaussian specimens. The parameters estimate was obtained through application of the Maximum Likelihood Principle.

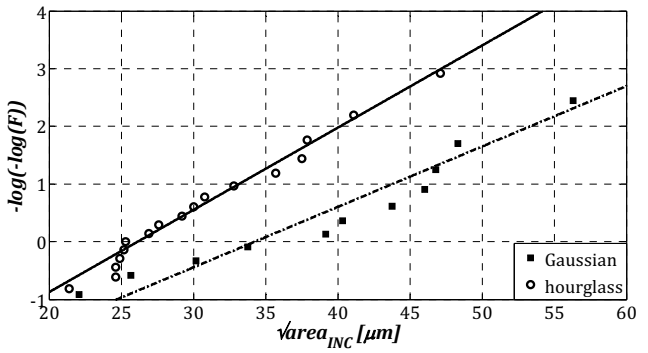

Fig. 6: Gumbel plot showing fitting of experimental data obtained by testing hourglass and Gaussian specimens.

According to Fig. 6, inclusions from which failure originated are significantly larger in Gaussian specimens than in hourglass specimens. The percentage of inclusions with larger size is different: two out of seventeen (12%) inclusions are larger than 40μm in hourglass specimens, while six out of eleven inclusions (about 55%) are larger than 40μm in Gaussian specimens. Moreover, the largest inclusion in Gaussian specimens (56μm) is about 19% larger than the largest inclusion in hourglass specimens (47μm). The different VHCF strength is therefore justified by the different size of inclusions present in the two specimen types. According to Fig. 6, large inclusion are rarer in the limited RV of hourglass specimen. On the other hand, the increment of the RV obtained through Gaussian specimens increases the probability of finding inclusions with larger size and, as a consequence, induce a reduction of the VHCF strength.

Conclusions

Ultrasonic tests were carried out on hourglass specimens with a limited RV ($200\,mm^3$) and on Gaussian specimens with a large RV ($2300\,mm^3$) in order to assess the influence of the SE factor in the VHCF regime. Experimental results showed that the VHCF response is significantly affected by the specimen RV. In particular, hourglass specimens exhibit the largest VCHF limit and strength at 10^{10} cycles. The different inclusion dimension can be considered as the main reason for the different VHCF response obtained by testing hourglass and Gaussian specimens: inclusions with a larger size are rarer in limited RVs, thus inducing a significant increment of the VHCF strength.

Acknowledgements

The authors would like to thank the research group of Prof. D. Firrao for the valuable suggestions concerning the material choice and the applied heat treatments.

References

[1] C. Bathias, P.C. Paris, Gigacycle fatigue in mechanical practice. CRC Dekker, New York, 2005.
[2] S. Stanzl-Tschegg, Very high cycle fatigue measuring techniques, Int. J. Fatigue 60 (2014) 2-17.
[3] H. Mughrabi, On 'multi-stage' fatigue life diagrams and the relevant life-controlling mechanisms in ultrahigh-cycle fatigue, Fatigue Fract. Eng. Mater. Struct. 25 (2002) 755-764.

[4] D.S Paolino, G. Chiandussi, M. Rossetto, A unified statistical model for S-N fatigue curves: probabilistic definition, Fatigue Fract. Eng. Mater. Struct. 36 (2013), 187-201.
[5] Y. Furuya, Specimen size effects on gigacycle fatigue properties of high-strength steel under ultrasonic fatigue testing, Scripta Mater. 58 (2008) 1014–1017.
[6] Y. Furuya, Size effects in gigacycle fatigue of high-strength steel under ultrasonic fatigue testing, Procedia Eng. 2 (2010) 485–490.
[7]Y. Furuya, Notable size effects on very high cycle fatigue properties of high strength steel, Mater. Sci. Eng. A 528 (2011) 5234–5240.
[8] Y. Murakami, Metal Fatigue: Effects Of Small Defects And Nonmetallic Inclusions. Elsevier, Oxford, 2002.
[9] D.S. Paolino, A. Tridello, G. Chiandussi, M. Rossetto, On specimen design for size effect evaluation in ultrasonic gigacycle fatigue testing, Fatigue Fract. Eng. Mater. Struct. 5 (2014) 570-579.
[10] D.S. Paolino, A. Tridello, G. Chiandussi, M. Rossetto, Comparison between dog-bone and Gaussian specimens for size effect evaluation in gigacycle fatigue, Frattura e Integrità Strutturale 26 (2013) 49-56.
[11] D.S. Paolino, M. Rossetto, G. Chiandussi , A. Tridello, Sviluppo di una macchina a ultrasuoni per prove di fatica gigaciclica. Proceedings of the 41th AIAS Conference, Vicenza 2012 (In Italian).
[12] Y. Murakami, N. N. Yokoyama, J. Nagata, Mechanism of fatigue failure in ultralong life regime, Fract. Eng. Mater. Struct. 25 (2002) 735-746.